RANS simulations of rotating flows

By G. Iaccarino, A. Ooi, B. A. Pettersson Reif AND P. Durbin

1. Motivation and objectives

Numerous experimental and numerical investigations have established that body forces arising from imposed system rotation or from streamline curvature can substantially alter both the mean flow field and the intensity and structure of the turbulence. The most natural level of closure modeling to adopt in these cases is second-moment closure (SMC), which in a natural and systematic manner accounts for rotation. The potential advantage of SMC stems from the appearance of exact production terms due to mean flow gradients and system rotation. The full SMC equations also contain convective and dispersive transport of the second moments. This modeling approach is physically more appealing than the eddy-viscosity concept, but it is still not tractable in complex applications due to excessive computational cost and to computational stiffness.

The most frequently adopted turbulence closures in industrial computations invoke the linear eddy-viscosity hypothesis for the mean flow and scalar transport equations for the turbulence — e.g., the $k-\varepsilon$ model. An inherent shortcoming of these models is their property of material frame indifference; in other words, they are independent of imposed system rotation.

Common practise to sensitize RANS models to noninertial effects is to modify the turbulent length scale by adding rotation dependent terms to the dissipation rate equation (Howard *et al.* 1980). Although the dissipation rate model equation is based more on intuition than on rigorous arguments, it still exhibits a surprising degree of generality. Therefore, a reluctance exists to introduce *ad hoc* rotation terms into the ε transport equation.

A different approach to sensitize the eddy-viscosity model to the effect of system rotation is based on the work by Gatski & Speziale (1993). They derived an explicit solution to the Algebraic Stress representation of a linear SMC in a noninertial frame of reference by the integrity basis technique. The coefficient of the linear term in their explicit solution is a function of the nondimensional velocity gradients invariants:

$$\eta_1 = S^*_{ik}S^*_{ik}, \eta_2 = W^*_{ik}W^*_{ik} \tag{1}$$

where:

$$S^*_{ik} = T/2\left(\frac{\partial U_i}{\partial x_k} + \frac{\partial U_k}{\partial x_i}\right) \tag{2}$$

$$W^*_{ik} = T/2\left[\left(\frac{\partial U_i}{\partial x_k} - \frac{\partial U_k}{\partial x_i}\right) + 4.5\epsilon_{kim}\Omega_m\right] \tag{3}$$

and T is the turbulent time scale.

Similarly, Petterson *et al.* (1999) sensitized the $\overline{v^2} - f$ linear model (Durbin, 1993) to effects of system rotation and streamline curvature by expressing the eddy-viscosity coefficient as a function of the invariants (1), $C_\mu^* = C_\mu^*(\eta_1, \eta_2)$. Gatski & Speziale's (1993) solution for rotating flow and the bifurcation diagram (Durbin & Petterson, 1999) were used to guide the development of this function.

The *only* modification to the original model (Durbin, 1993) consists in a change of the eddy viscosity,

$$\mu_t = C_\mu^* \overline{v^2} T. \tag{4}$$

Instead of C_μ^* being a constant, it is given by

$$C_\mu^* = C_\mu \frac{1 + \alpha_2|\eta_3| + \alpha_3\eta_3}{1 + \alpha_4|\eta_3|} \left(\sqrt{\frac{1 + \alpha_5\eta_1}{1 + \alpha_5\eta_2}} + \alpha_1\sqrt{\eta_2}\sqrt{|\eta_3| - \eta_3} \right)^{-1} \tag{5}$$

where $\eta_3 = \eta_1 - \eta_2$ and C_μ retains its original value. The free coefficients α_i are determined with reference to the bifurcation diagram and are given by

$$\alpha_1 = 0.055\sqrt{f_1}, \alpha_2 = \frac{1}{2}f_1, \alpha_3 = \frac{1}{4}f_1, \alpha_4 = \frac{1}{5}\sqrt{f_1}\alpha_5 = \frac{1}{40} \tag{6}$$

where $f_1 = \sqrt{(\overline{v^2}/k)/(\overline{v^2}/k)_\infty}$. The modified $\overline{v^2} - f$ model retains the linear eddy-viscosity assumption (4) and reduces to its original form in parallel shear flows in an inertial frame of reference. The derivation of this formulation can be found in Durbin & Petterson (1999).

2. Results

In order to assess the performance of the modified $\overline{v^2} - f$ model, three test cases are considered. These cases were selected with the objective to test the model in flows in which the turbulence field dominates the overall effect of imposed body forces. The success of the predictions, therefore, relies heavily on the turbulence closure. Model predictions are compared with available experimental and DNS data as well as with results obtained with the original $\overline{v^2} - f$ model and with a SMC model (Speziale *et al.*, 1991).

2.1 Rotating channel flow

The most frequently used test case for assessing turbulence closures in a rotating frame is fully developed channel flow in orthogonal mode rotation (Fig. 1). This configuration has been the subject of a number of experimental and numerical studies (Johnston *et al.* 1972, Kristoffersen & Andersson 1993). Depending on the sense of rotation, the pressure-driven flow in the channel is subjected to stabilization or destabilization of the turbulence; if the rotation vector Ω is parallel (antiparallel) to the background mean flow vorticity, the turbulence is stabilized (destabilized). The imposed rotation breaks the symmetry of the flow field and may eventually lead to relaminarization on the stable side of the channel. A salient feature of this

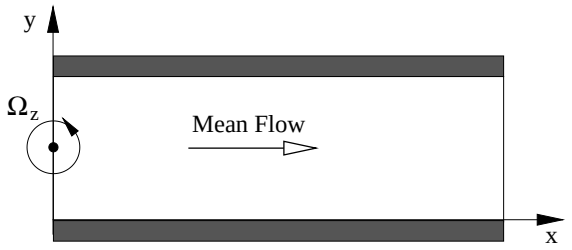

FIGURE 1. Rotating Channel Flow - Sketch of the problem.

particular flow is that the rotational effects on the mean flow field enter *only* via the turbulence equations.

Model predictions are compared to the DNS data reported by Kristoffen & Andersson (1993) at $Re_\tau = 194$ and $Ro = 2h\Omega/U_b = 0.1$, where U_b is the bulk velocity and Ω the rotational velocity.

The mean velocity distributions across the channel displayed in Fig. 2a show the characteristic asymmetry caused by the imposed rotation. The model predictions are in close agreement with the DNS, and it is especially encouraging that the model is capable of reproducing the almost irrotational core region in which $dU/dy \sim 2\Omega$. By comparison, the original model returns the symmetric solution ($Ro = 0.0$) irrespective of Ro. It should also be recalled that the present and original models are identical at $Ro = 0.0$. The computed turbulence intensity on the stable side of the channel is reduced as shown in Fig. 3b; it agrees well with the DNS and SMC results although the stabilizing effect of the imposed rotation seems to be underpredicted.

The discrepancies between SMC results and the DNS data are largely due to the near-wall modeling adopted for the SMC model; it is a two layer formulation in which the turbulent dissipation, ϵ, is expressed in terms of the turbulent kinetic energy.

2.2 Rotating backstep

The flow over a backward facing step is characterized by the simultaneous presence of high shear and streamline curvature in the free shear layer immediately downstream the step. The strained and highly turbulent flow field reattaches further downstream. Rothe (1975) conducted an experimental study of a backstep flow in orthogonal mode rotation. This added the impact of the Coriolis force on the flow field. The experiments revealed a strong correlation between the imposed system rotation and the reattachment length. Nilsen & Andersson (1990) pointed out that the profound effects of rotation could mainly be attributed to changes in the turbulence field. The rotating backstep diffuser studied by Rothe (1975), therefore, is adopted in the present study to assess the model performance in a complex geometry.

The backstep diffuser, with the ratio of downstream channel height to the step height (h) of 2, was subjected to a constant angular velocity Ω about the z-axis parallel to the step (Fig. 3).

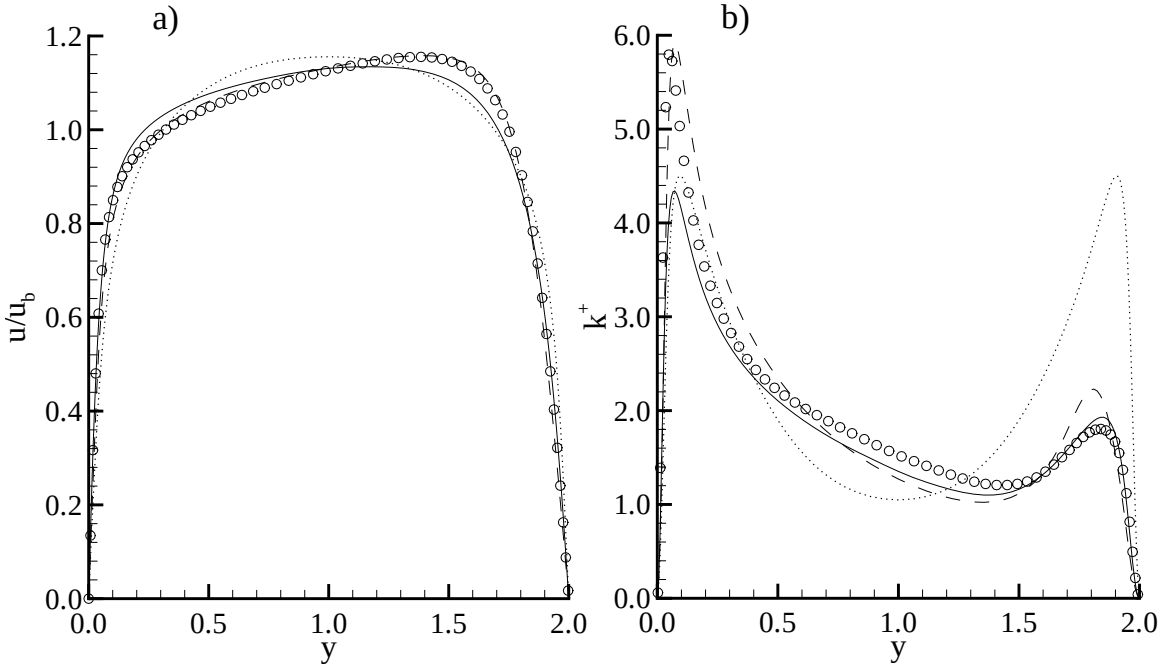

FIGURE 2. Rotating Channel Flow - Results: (a) velocity profile (b) turbulent kinetic energy; ∘ DNS; ——— SMC; – – – – modified $\overline{v^2} - f$; ····· original $\overline{v^2} - f$.

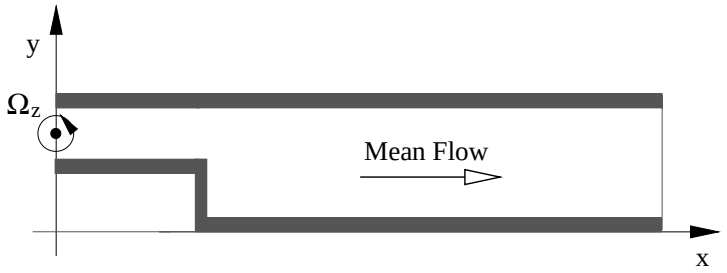

FIGURE 3. Rotating Backstep Flow - Sketch of the problem.

The inlet condition (four step heights upstream the step, $x/h = -4$) was prescribed from model computations of fully developed channel flow subjected to spanwise rotation. A 190×110 nonuniform grid was used for all calculations. This has proved to be sufficient to ensure grid independence.

Model predictions at Reynolds numbers $Re \equiv U_b h/\nu = 10^4$ and different rotation numbers $Ro \equiv \Omega h/U_b$ are compared with the experiments. Here, $Ro > 0$ is termed *destabilizing* rotation since the turbulence intensity on the stepped wall upstream the step tends to be enhanced. $Ro < 0$ is referred to as *stabilizing* rotation. The only measurement reported by Rothe (1975) is the variation of reattachment length with Ro. This makes the comparison largely qualitative. Results obtained by Nilsen & Andersson (1990) with a more elaborate implicit algebraic stress model (ASM) are also included.

Figure 4 compares the predicted reattachment length as a function of Ro with

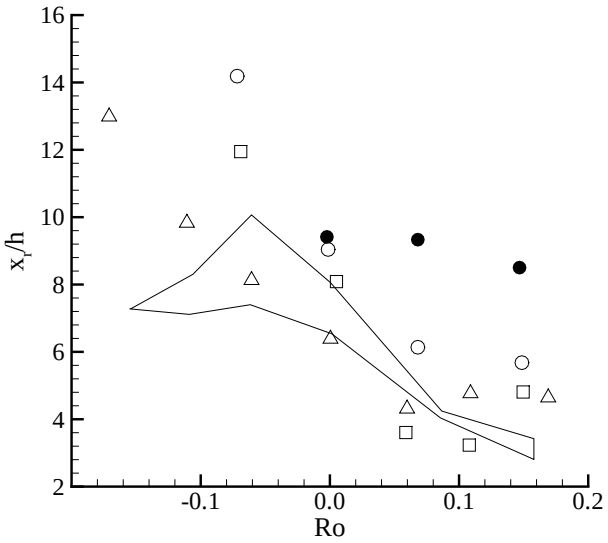

FIGURE 4. Rotating Backstep Flow - Results: Reattachment length closed area: experiments ($3.0x10^3 < Re < 2.8x10^4$); ▫ SMC; ▵ ASM ($Re = 5500$); ∘ modified $\overline{v^2} - f$; • original $\overline{v^2} - f$.

the experiments, SMC, and ASM results. The predictions using the present model compare well with the reference data for destabilizing rotation although the reattachment length in general is somewhat over predicted. Differences between SMC and $\overline{v^2} - f$ results are probably due to the different modeling of the near wall turbulence as discussed in the previous section. The differences between the present predictions and the ASM results seem partly to be an Re effect. It is noteworthy that the model captures the saturation of the rotational effect for sufficiently strong positive rotation as indicated by both the SMC and ASM results. The effect of stabilizing rotation is, however, too strong. For $Ro < 0$, the experimental results in Fig. 4 show a saturation of the rotational effect on the reattachment length that is qualitatively different from all the model predictions.

Figure 5 displays computed streamlines for different rotation numbers at $Re \approx 10^4$. The intensity of the main recirculation region increases for destabilizing rotation ($Ro > 0$) at the same time as its extent decreases. The length of the main recirculation zone is significantly increased by stabilizing rotation, but its intensity is hardly altered. Figure 5d also shows that a recirculation zone on the upper wall ($y/h = 2$) has developed ($2 \leq x/h \leq 8$) at high destabilizing rotation. It should be noted that the turbulence intensity along the upper wall tends to be reduced for $Ro > 0$.

Finally, it should be noted that the original $\overline{v^2} - f$ model predicts approximately the same reattachment length independent of imposed rotation. Since this model only responds to system rotation indirectly through changes to the mean flow field,

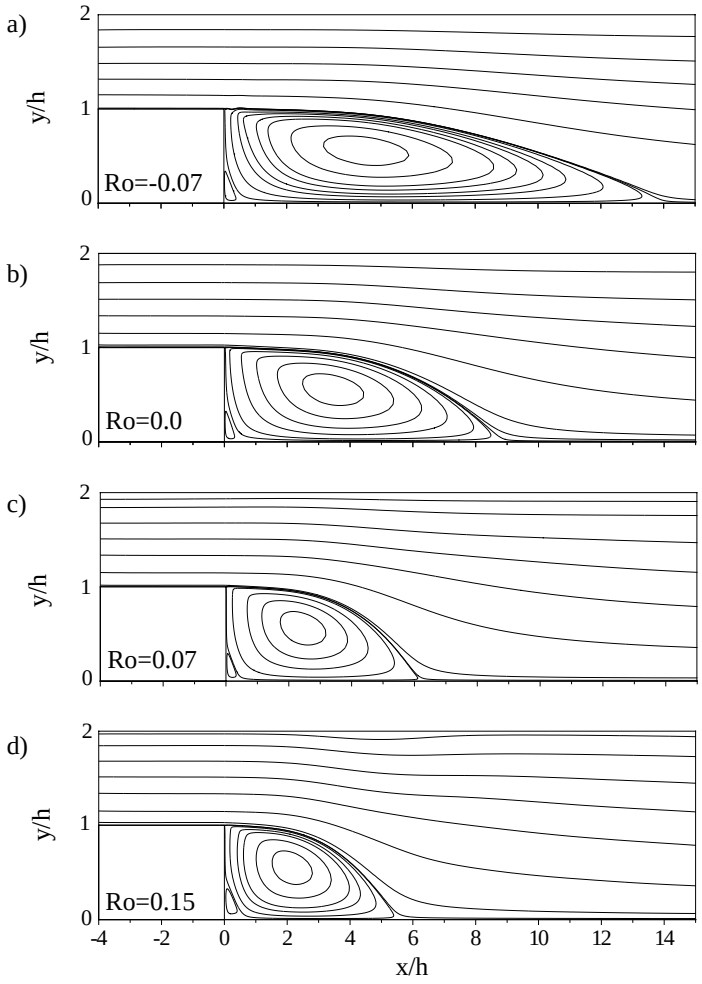

FIGURE 5. Rotating Backstep Flow - Results: Streamlines at different rotation number.

it can be concluded that the strong correlation between system rotation and reattachment length can be attributed to changes in the turbulence field. This is fully consistent with the findings of Nilsen & Andersson (1990).

2.3 Rotating cavity

The cylindrical cavity between two rotating disks and a peripheral shroud (Fig. 6) provides a convenient model geometry to study the flow structure in a practical gas turbine engine. Air enters the cavity axially through a central hole in the upstream disk and is deflected after impinging on the downstream disk; then, it exits through a thin layer adiacent to the outer shroud. The flow is characterized by a toroidal vortex located close to the upstream disk and, depending on the rotational velocity, by the establishment of two (symmetric) Ekman layers on the disks.

A 200×150 nonuniform grid was used for all calculations. The flow conditions are characterized by the rotation number $Ro \equiv \Omega s/U_i$ and the Reynolds numbers $Re \equiv U_i s/\nu$, where s is the disk spacing and U_i the inlet velocity. Two different flow conditions are considered, namely $Ro = 0.7, Re = 11000$ and $Ro = 2, Re = 4000$.

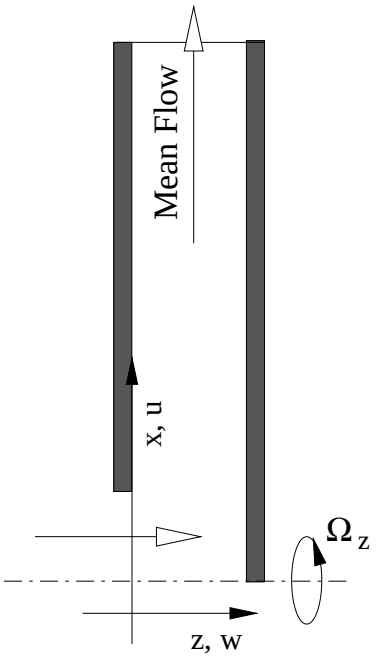

FIGURE 6. Rotating Cavity - Sketch of the problem.

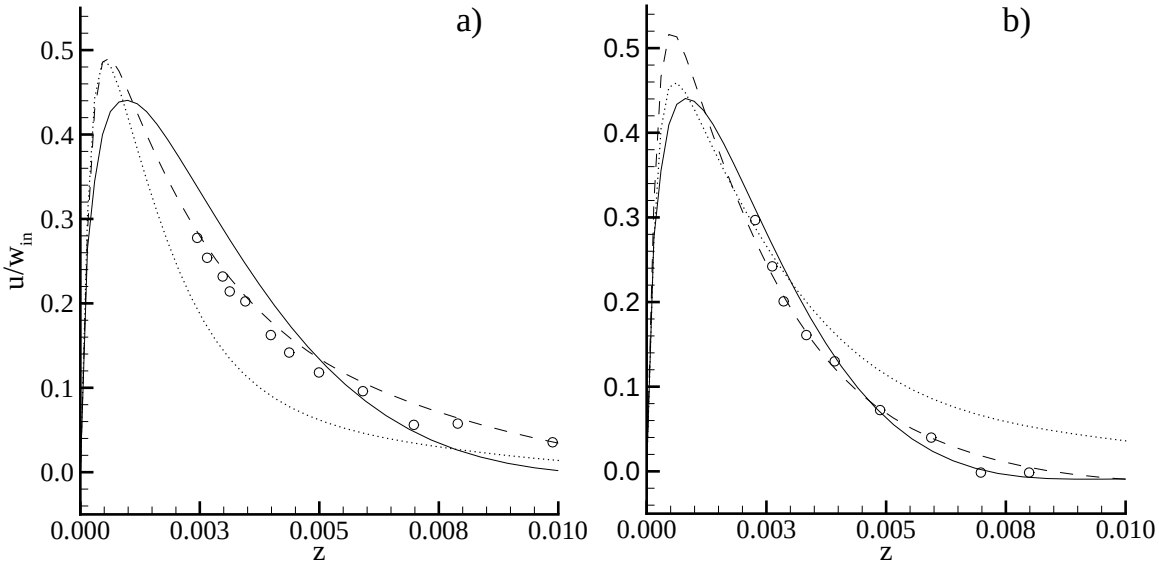

FIGURE 7. Rotating Cavity - Results: (Re = 11000, Ro = 0.7) radial velocity profile at x/b = 0.633 (a) and x/b = 0.833 (b); ∘ experiments; —— SMC; - - - - modified $\overline{v^2} - f$; ····· original $\overline{v^2} - f$.

These conditions correspond to the experimental measurements of Pincombe (1983).

Figures 7 and 8 show the radial velocity profiles in the boundary layer of the upstream disk using the $\overline{v^2} - f$ model for the two conditions considered. The results are compared to the experimental data as well as to SMC computations.

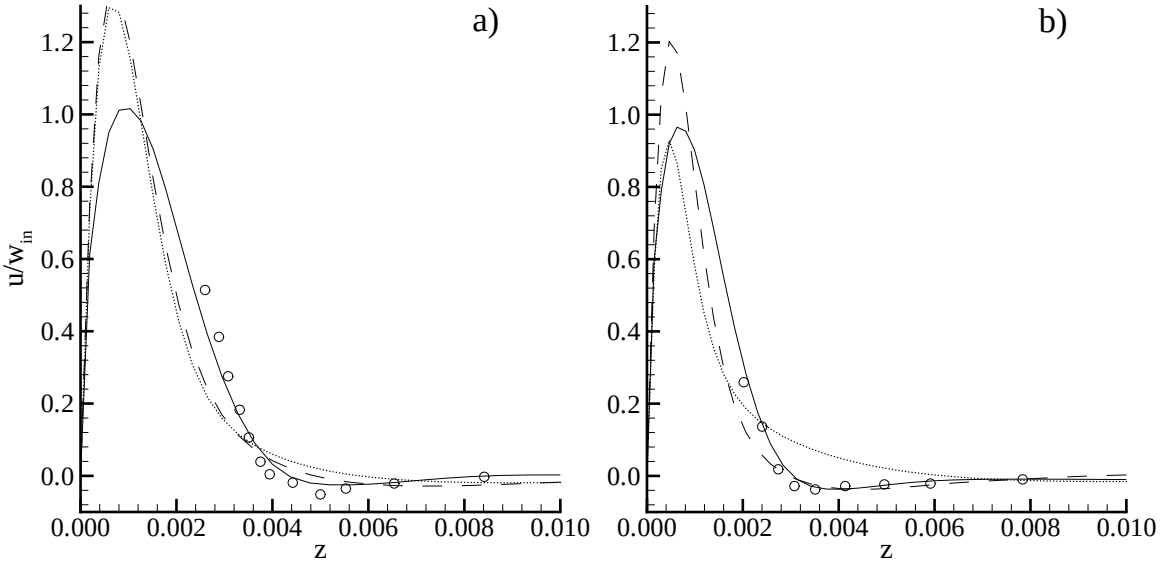

FIGURE 8. Rotating Cavity - Results: ($Re = 4000$, $Ro = 2.1$) radial velocity profile at $x/b = 0.633$ (a) and $x/b = 0.833$ (b); ∘ experiments; —— SMC; - - - - modified $\overline{v^2} - f$; ····· original $\overline{v^2} - f$.

The new model correctly predicts the presence of a recirculation cell between the disks; the location of the velocity inversion is also very well predicted at both rotation numbers.

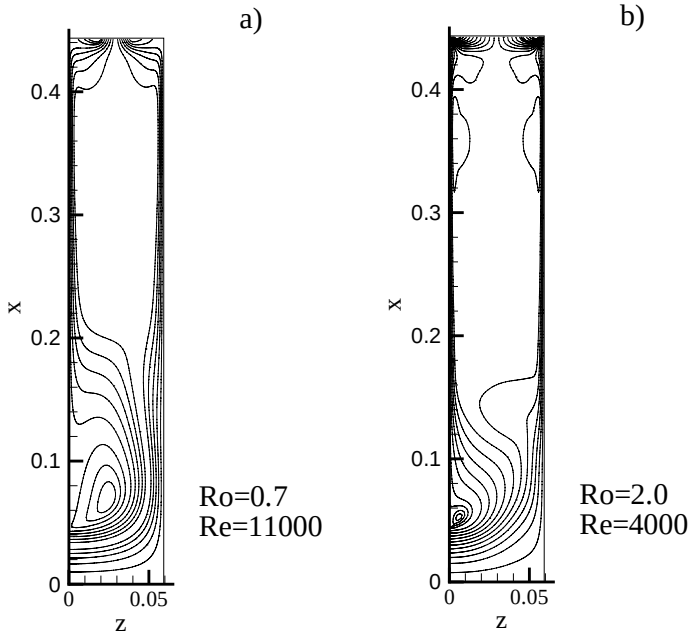

FIGURE 9. Rotating Cavity - Results: Streamlines at different rotation number.

Associated streamlines are reported in Fig. 9 and can be compared to those presented in Morse (1991). The flow impinges on the downstream disk giving rise to a strong wall-jet while a vortex ring is formed close the upstream disk; by increasing the rotation number, the wall jet weakens and two symmetric Ekman layers are formed on the rotating disks.

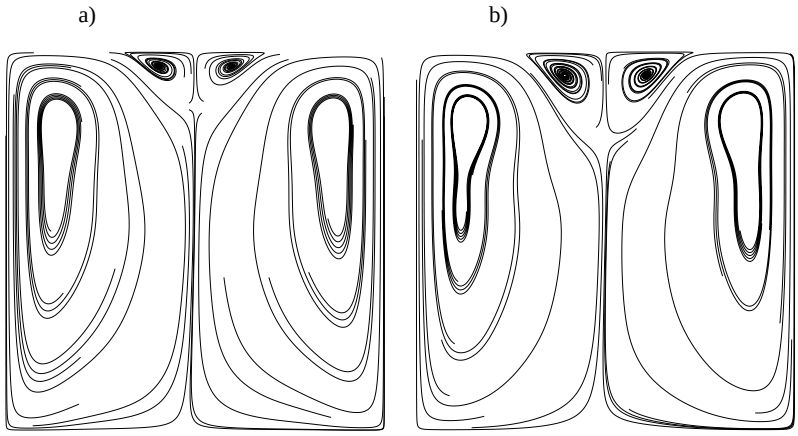

FIGURE 10. Rotating Square Duct - Results: Streamlines in a cross-section; (a) modified $\overline{v^2} - f$, (b) SMC.

The original model responds to the rotation only through the modification of the mean velocity fields and, at low rotation number, is unable to predict the reverse velocity on the upstream disk (Fig. 7).

3. Future plans

In the present study, the $\overline{v^2} - f$ model has been applied to flows with rotational effects. The original model was modified to account for the frame rotation by introducing a coefficient depending on the velocity gradient invariants into the definition of the eddy viscosity.

Three different test cases were used to assess the performance of the model: (*i*) fully developed channel flow in orthogonal mode rotation, (*ii*) a rotating backstep diffuser, and (*iii*) a rotating cavity.

Comparison between experimental data and SMC results confirm that the modified model performs well in the prediction of the effects of rotation both on the mean flow and on the turbulent fields.

Future work will be devoted to the application of the modified model to the prediction of three-dimensional flows; preliminary results for the flow in a rotating square duct are reported in Fig. 10 in terms of flow patterns in a section of the duct. The agreement between the modified $\overline{v^2} - f$ and the SMC model is encouraging.

REFERENCES

Durbin, P. A. 1993 A Reynolds stress model for near-wall turbulence. *J. Fluid Mech.* **249,** 465-498.

Gatski, T. B. & Speziale, C. G. 1993 On explicit algebraic stress models for complex turbulent flows. *J. Fluid Mech.* **254,** 59-78.

Howard, J. H. G., Patankar, S. V. & Bordynuik, R. M. 1980 Flow prediction in rotating ducts using Coriolis-modified turbulence models. *ASME J. Fluids Eng.* **102,** 456-461.

Johnston, J. P., Halleen, R. M., & Lezius, D. K. 1972 Effects of spanwise rotation on the structure of two-dimensional fully developed turbulent channel flow. *J. Fluid Mech.* **56,** 533-557.

Kristoffersen, R. & Andersson, H. I. 1993 Direct simulations of low-Reynolds-number turbulent flow in a rotating channel. *J. Fluid Mech.* **256,** 163-197.

Morse, A. P. 1991 Application of a low Reynolds number $k-\epsilon$ turbulence model to high-speed rotating cavity flows. *ASME J. Turbomach.* **113,** 98-113.

Nilsen, P. J. & Andersson, H. I. 1990 Rotational effects on sudden-expansion flows. *Eng. turbulence modeling and experiments.* Elsevier Science Pub. Co., 65-72.

Pettersson Reif, B. A., Durbin, P. A., & Ooi, A. 1999 Modeling rotational effects in eddy-viscosity closures. *Int. J. Heat Fluid Flow* (to appear).

Pincombe, J. R. 1983 Optical measurements of the flow inside rotating cylinder. *Ph.D. Thesis,* University of Sussex, UK.

Rothe, P. H. 1975 The effects of system rotation on separation, reattachment and performance in two-dimensional diffusers. *Stanford University Dissertation,* Dept. Mechanical Engineering.

Speziale, C. G., Sarkar, S., & Gatski, T. B., 1991 Modeling the pressure-strain correlation of turbulence: an invariant dynamical systems approach. *J. Fluid Mech.* **227,** 227-245.